EBioMedicine 44 (2019) 419–430

Contents lists available at ScienceDirect

EBioMedicine

journal homepage: www.ebiomedicine.com

EBioMedicine
Published by THE LANCET

Research paper

The BET inhibitor JQ1 attenuates double-strand break repair and sensitizes models of pancreatic ductal adenocarcinoma to PARP inhibitors

Aubrey L. Miller [a], Samuel C. Fehling [a], Patrick L. Garcia [a], Tracy L. Gamblin [a], Leona N. Council [b,c], Robert C.A.M. van Waardenburg [a], Eddy S. Yang [d], James E. Bradner [e,1], Karina J. Yoon [a,*]

[a] Department of Pharmacology and Toxicology, University of Alabama at Birmingham, 1670 University Blvd, Birmingham, AL, USA
[b] Department of Pathology, Division of Anatomic Pathology, University of Alabama at Birmingham, NP3551 North Pavilion UAB Hospital, Birmingham, AL, USA
[c] The Birmingham Veterans Administration Medical Center, 700 19th St S, Birmingham, AL, USA
[d] Department of Radiation Oncology, University of Alabama at Birmingham, Hazelrig Salter Radiation Oncology Center, 1700 6th Avenue S, Birmingham, AL, USA
[e] Department of Medical Oncology, Dana-Farber Cancer Institute, Harvard Medical School, Boston, MA, USA

ARTICLE INFO

Article history:
Received 11 April 2019
Received in revised form 14 May 2019
Accepted 14 May 2019
Available online 22 May 2019

Keywords:
BET bromodomain inhibitor (BETi)
Pancreatic cancer
PARP inhibitor (PARPi)
DNA repair and damage
Patient-derived xenograft model
DNA double-strand break repair proteins

ABSTRACT

Background: DNA repair deficiency accumulates DNA damage and sensitizes tumor cells to PARP inhibitors (PARPi). Based on our observation that the BET inhibitor JQ1 increases levels of DNA damage, we evaluated the efficacy of JQ1 + the PARPi olaparib in preclinical models of pancreatic ductal adenocarcinoma (PDAC). We also addressed the mechanism by which JQ1 increased DNA damage.

Methods: The effect of JQ1 + olaparib on *in vivo* tumor growth was assessed with patient-derived xenograft (PDX) models of PDAC. Changes in protein expression were detected by immunohistochemistry and immunoblot. *In vitro* growth inhibition and mechanistic studies were done using alamarBlue, qRT-PCR, immunoblot, immunofluorescence, ChIP, and shRNA knockdown assays.

Findings: Tumors exposed *in vivo* to JQ1 had higher levels of the DNA damage marker γH2AX than tumors exposed to vehicle only. Increases in γH2AX was concomitant with decreased expression of DNA repair proteins Ku80 and RAD51. JQ1 + olaparib inhibited the growth of PDX tumors greater than either drug alone. Mechanistically, ChIP assays demonstrated that JQ1 decreased the association of BRD4 and BRD2 with promoter loci of Ku80 and RAD51, and shRNA data showed that expression of Ku80 and RAD51 was BRD4- and BRD2-dependent in PDAC cell lines.

Interpretation: The data are consistent with the hypothesis that JQ1 confers a repair deficient phenotype and the consequent accumulation of DNA damage sensitizes PDAC cells to PARPi. Combinations of BET inhibitors with PARPi may provide a novel strategy for treating PDAC.

Fund: NIH grants R01CA208272 and R21CA205501; UAB CMB T32 predoctoral training grant.

1. Introduction

Pancreatic ductal adenocarcinoma (PDAC) is the most common type of pancreatic cancer, accounting for ~45,000 deaths annually in the United States [1]. Despite the use of aggressive chemotherapeutic regimens such as FOLFIRINOX, which supports a median survival of 11 months, the 5-year survival for patients with PDAC has remained at ~7% for the last 40 years [1,2]. Recently the bromodomain and extraterminal domain (BET) family of proteins has been investigated as a potentially effective therapeutic target for treating PDAC tumors. The four members of this family of proteins (BRD2, BRD3, BRD4, BRDT) function as scaffolds for the recruitment of transcriptional activators to promoter or super enhancer loci of genes whose transcription is regulated by RNA polymerase II [3]. BET proteins BRD2 and BRD3 promote PDAC cell proliferation and growth, likely by modulating the activity of members of the GLI family of transcription factors [4]. BRD4 promotes PDAC cell proliferation by affecting expression of proteins of the sonic hedgehog pathway [5]. Current literature indicates that JQ1 inhibits BET protein function by binding to the domain of BET that interacts directly with acetylated lysine residues on specific histones, thereby decreasing expression of proteins that rely on BET-dependent

* Corresponding author at: Department of Pharmacology and Toxicology, University of Alabama at Birmingham, VH 241, 1670 University Blvd, Birmingham, AL 35294, USA.
E-mail address: kyoon@uab.edu (K.J. Yoon).
[1] Current address: Novartis Institutes for Biomedical Research, Cambridge, MA, USA.

https://doi.org/10.1016/j.ebiom.2019.05.035

Research in context

Evidence before this study

The BET bromodomain proteins are transcriptional regulators that control expression of genes that contribute to tumor progression. We and others showed that pharmacological inhibition of this family of proteins suppresses tumor growth of models of several tumor types. However, even in preclinical models, BET inhibitors as single agents do not achieve durable responses. Three published studies assessed the efficacy of a BET inhibitor in combination with a PARP inhibitor. These studies reported synergy with this combination in homologous recombination (HR)-proficient ovarian, breast, and prostate cancer cells *in vitro*. The combination also decreased tumor progression in xenograft models of ovarian and breast cancer.

Added value of this study

This study investigated the effectiveness of combining the BET inhibitor JQ1 with a PARP inhibitor in several *in vitro* and *in vivo* pancreatic ductal adenocarcinoma (PDAC) models. Data in this report are the first to: 1) show synergy *in vitro* and efficacy *in vivo* ($p < .001$) of a BET inhibitor + a PARP inhibitor using models of PDAC; 2) demonstrate that this combination inhibits ($p < .001$) progression of independently derived, *KRAS* mutated patient-derived xenograft (PDX) models at nontoxic doses equivalent to those tolerated clinically; 3) document that JQ1 inhibits expression of not only the HR DNA repair protein RAD51 but also the non-homologous end joining (NHEJ) repair protein Ku80 in PDAC cells *in vitro* and tumors *in vivo*; 4) provide mechanistic data to confirm that expression of RAD51 and Ku80 is BRD2- and BRD4-dependent using ChIP and shRNA studies in PDAC cells. The work provides mechanistic and efficacy data that support assessing this combination in clinical trials for patients with PDAC.

Implications of all the available evidence

Together the data strongly suggest that combinations of BET + PARP inhibitors merit further evaluation for treatment of solid tumors. Our *in vivo* work suggests further that this combination may be particularly effective for treating PDAC.

mechanisms for transcription. We and others have demonstrated that JQ1 has anti-tumor efficacy in multiple models of pancreatic cancer [6–8]. However, in those studies JQ1 did not induce complete remissions as a single agent, leading us to consider agents that might be combined with BET inhibitors to maximize anti-tumor response.

In this study, we examined the mechanism of BET inhibitor-induced DNA repair deficiency and combined the BET inhibitor JQ1 with a PARP inhibitor (PARPi, veliparib or olaparib) and evaluated the efficacy of these combinations in several PDAC models. The role of BET proteins in transcriptional activation is well established [9]. Recent work indicates that BRD4 may inhibit DNA damage response signaling and irradiation-induced H2AX phosphorylation through effects on chromatin structure [10]. BRD4 also contributes to non-homologous end joining (NHEJ) repair during immunoglobulin class switch recombination [11]. In a given cell type, inhibition of BRD4 function might inhibit or promote DNA repair and affect levels of DNA damage; but studies addressing the effect of BET inhibitors on overall DNA damage in PDAC have not been reported.

Relevant to the question of identifying agents with which JQ1 might be effectively combined, it is known that PARP inhibitors have greatest efficacy in tumor cells deficient in homologous recombination (HR) DNA repair or in combination with agents that induce DNA damage [12–17]. We have shown that JQ1 increases levels of H2AX phosphorylation *in vitro* and *in vivo*, indicating that JQ1 increases DNA damage. Therefore, we evaluated the impact of JQ1, a PARPi (veliparib or olaparib), and the combination on DNA damage, apoptosis, DNA double-strand break repair protein levels and PDAC tumor cell viability *in vitro* and *in vivo*. We also addressed the mechanism by which JQ1 effects DNA damage and repair.

2. Materials and methods

2.1. Ethics statement

Animal protocols were approved by the University of Alabama at Birmingham Institutional Animal Care and Use Committee (IACUC-09186 and IACUC-20569).

2.2. Cell lines and compounds

Panc1, BxPC3, and MiaPaCa2 pancreatic cancer cells were purchased from the American Type Culture Collection (Manassa, VA, USA). Cells were cultured under recommended conditions. All cell lines were authenticated by short tandem repeat DNA profiling at the UAB Heflin Center for Genomic Science (Birmingham, AL, USA). All pancreatic cancer cell lines used were tested for mycoplasma using MycoAlertTM PLUS Mycoplasma Detection Kit (Lonza, Walkersville, MD, USA) and results were negative. Olaparib (HY-10162, MedChem Express, Monmouth Junction, NJ, USA), JQ1 (a generous gift from Dr. Bradner; HY-13030, MedChem Express), and veliparib (a generous gift from Dr. Yang; ABT-888, Enzo Life Sciences, Farmingdale, NY, USA) were dissolved in DMSO.

2.3. Immunoblot analysis

Cell and tumor lysates were prepared in NP-40 lysis buffer with protease inhibitor cocktail or Cell Lysis Buffer (Cell signaling, Danvers, MA, USA) respectively. Analysis of lysates was carried out as previously described [7]. Primary antibodies used were: γH2AX (Cell Signaling), RAD51 (abcam, Cambridge, MA, USA), Ku80 (Bethyl Laboratories, Montgomery, TX, USA), BRD4 (Cell Signaling), BRD2 (Cell Signaling), vinculin (Santa Cruz Biotech, Dallas, TX, USA), GAPDH (Cell Signaling), β-actin (Cell Signaling), α-Tubulin (Cell Signaling), p21 (Cell Signaling), Cleaved PARP (Cell Signaling). Blots were quantitated using ImageStudio Lite (LI-COR Biosciences, Lincoln, NE, USA).

2.4. Immunohistochemistry

Immunohistochemistry staining was performed as previously described [7]. Ki67 and γH2AX indices: 10 random high magnification fields were taken, positive tumor cells counted and divided by the total number of tumor cells in two independent experiments. Expression indices were calculated by assessing each field of stained tumor tissue, and assigning a staining intensity (0, 1, 2, 3) to a given percent of tumor cells. The percentage was multiplied by the staining intensity and then these values were added to calculate a score between 0 and 300. Primary antibodies: Ki67 (abcam), γH2AX (Cell Signaling), cleaved caspase 3 (Cell Signaling), RAD51 (abcam), Ku80 (Bethyl Laboratories).

2.5. Histological analysis

Histological analysis was performed as previously described [7]. Photomicrographs were taken on an Olympus BH-2 microscope with DP71 camera and DPS-BSW v3.1 software (Center Valley, PA, USA).

2.6. In vitro cell viability assay

Cell viability assays were carried out as previously described [7]. Briefly, cells were seeded in 96 well plates. Serial dilutions of JQ1 and/or PARPi were added to the culture medium for 72 h. AlamarBlue reagent was applied according to the directions of the manufacturer, and fluorescence read on a Victor X5 microplate reader at 590 nm.

2.7. In vivo inhibition of tumor growth

Female 4-week old SCID CB $17^{-/-}$ mice were purchased from Taconic Farms (Newton, MA, USA) and housed in the AAALAC accredited vivarium at UAB Research Support Building. Development and characterization of the PDAC patient-derived xenografts (UAB-PA4 and UAB-PA16) have been previously described [18]. Mice bearing bilateral tumors were randomized into four groups of 5 mice/group (except vehicle control for UAB-PA4 [4 mice/group]) when tumors reached ~200 mm^3. Mice received intraperitoneal injections of vehicle (10% DMSO in 10% β-cyclodextrin x 2 injections), 50 mg/kg JQ1, 50 mg/kg olaparib, or the combination (50 mg/kg olaparib followed by 50 mg/kg JQ1) daily for 21 days. Drugs were prepared as instructed by the manufacturer. Tumor size was measured every other day using digital calipers, and tumor volume calculated using the formula $v = (\pi/6)\ xd^3$. Twenty-four hours following final treatment mice were euthanized. Tumor tissue was harvested, formalin fixed and paraffin embedded or snap frozen in liquid nitrogen for further analysis. All values are presented as mean ± S.E.M. Tumor volumes were compared using two-way analysis of variance (ANOVA) using GraphPad Prism (version 7).

2.8. Immunofluorescence

Cells were seeded in chamber slides, and treated for 24 h. Cells were fixed in 10% NBF for 10 min, and permeabilized with 0.01% Triton X-100 for 10 min. Non-specific antibody binding was minimized by blocking in 2% BSA for 1 h. Cells were then incubated at 4 °C overnight with antibody anti-γH2AX (MilliporeSigma, Burlington, MA, USA) or anti-RAD51 (abcam). Cells were incubated with secondary antibody Alexa Fluor goat anti-rabbit (or -mouse) 488 (Fisher Scientific, Waltham, MA, USA) for 1 h at room temperature. Coverslips were mounted using ProLong Gold Antifade Reagent with DAPI (Cell Signaling). Immunofluorescent staining was visualized using the Zeiss Axio Observer Z.1 microscope with the Zen 2011 Blue imaging software.

2.9. Clonogenic assays

Panc1 cells were plated at 200 cells/well in 24 well plates. Cells were then exposed to DMSO, JQ1 (1 μM), olaparib (1 μM), or the combination for 72 h. Drug-containing media was then removed, cells washed with PBS and overlaid with drug-free medium. On day 14, cells were fixed with 10% NBF and stained with 0.025% crystal violet. Cell groupings comprised of at least 50 cells were considered colonies. Two independent experiments were performed.

2.10. RNA isolation and qRT-PCR

Total RNA was isolated using TRIzol-chloroform extraction. qRT-PCR analysis was performed as previously described [7]. Primers used are listed in Table S1.

2.11. Chromatin immunoprecipitation (ChIP)

ChIP was performed using the SimpleChIP Plus Kit (Cell Signaling). Digested cellular chromatin was immunoprecipitated with a ChIP grade anti-BRD4 or anti-BRD2 antibody (Cell Signaling) or normal Rabbit IgG (Cell Signaling) used as the negative control. Levels of DNA sequences that co-precipitated with BRD4 or BRD2 were quantitated using qRT-PCR with primers that flanked regions of the Ku80 and RAD51 promoter loci marked by H3K27 acetylation. Data were analyzed relative to the percent input (2%) and then normalized to DMSO control. A minimum of two independent experiments were performed. Primers used are listed in Table S1.

2.12. Vectors and cell transfectants

BxPC3 and Panc1 cells were transfected with MISSION shRNA (MilliporeSigma) targeted for BRD4, BRD2 or the control shRNA for GFP (Addgene, Watertown, MA, USA) using PEI (Polysciences Inc., Warrington, VA, USA). After 8 h transfection, media was removed and regular medium was added and cells were allowed to recover for an additional 72 h. Stable transfectants were selected with media containing 10 μg/mL of puromycin (Enzo Life Sciences). The shRNA oligos used are listed in Table S1.

2.13. Statistical analysis

All statistical analyses were performed using GraphPad Prism 7 (San Diego, CA, USA). Unless otherwise specified statistical significance was calculated using the one-way ANOVA. $p < .05$ was considered significant.

3. Results

3.1. JQ1 increased the level of the DNA damage marker γH2AX in PDAC cells and tumors

BET proteins are essential for chromatin remodeling during the DNA damage response, and inhibition of BET protein function modifies chromatin structure and induces cell cycle arrest [3,10,19]. We hypothesized that BET inhibition would also minimize DNA repair. We addressed this hypothesis by exposing PDAC cells to the BET inhibitor JQ1 *in vitro* or *in vivo* and assessed levels of DNA damage as reflected by protein level and number of cells with detectable foci of the phosphorylated Ser-139 variant of histone H2AX (γH2AX), an early cellular response to DNA strand breaks and a marker for DNA damage [20]. Immunofluorescence (IF) and immunoblot (IB) data using an antibody specific for γH2AX demonstrated that JQ1 increased the level of γH2AX *in vitro* and *in vivo* (Fig. 1). IF data demonstrated JQ1 increased γH2AX foci in BxPC3 PDAC cells, in a dose-dependent manner ($p < .05$, one-way ANOVA) (Fig. 1a). IB data showed that the increase in γH2AX levels was not unique to BxPC3 cells, as JQ1 also increased γH2AX in Panc1 and MiaPaCa2 PDAC cells in a dose-dependent manner (Fig. 1b, c).

In vivo data were consistent with *in vitro* results. To first confirm that JQ1 increased DNA damage *in vivo* as well as *in vitro* at efficacious tolerated doses [7], we immunostained tumor tissue harvested 24 h following termination of treatment of vehicle control (VC) mice or mice treated with JQ1 50 mg/kg daily for 21 or 28 days, for levels of γH2AX (Fig. 1d). Results are presented as percent of tumor cells positive for γH2AX, and demonstrate that JQ1 *in vivo* increased γH2AX levels in UAB-PA3, -PA4, -PA10, and -PA30 tumors (Fig. 1e). The data show the novel observation that JQ1 accumulated DNA damage *in vivo* ($p < .001$, Student's *t*-test) as well as *in vitro* ($p < .05$, one-way ANOVA) in this tumor type.

3.2. JQ1 inhibited expression of DNA repair proteins Ku80 and RAD51 in PDAC cells

The BET protein BRD4, one of the principal targets of JQ1, facilitates gene expression and recruits DNA repair components such as 53BP1 to sites of DNA double-strand breaks to facilitate repair [11]. We hypothesized that the observed JQ1-induced increase in γH2AX, might not only regulate recruitment of repair components to sites of damaged DNA but might also decrease expression of specific DNA repair genes.

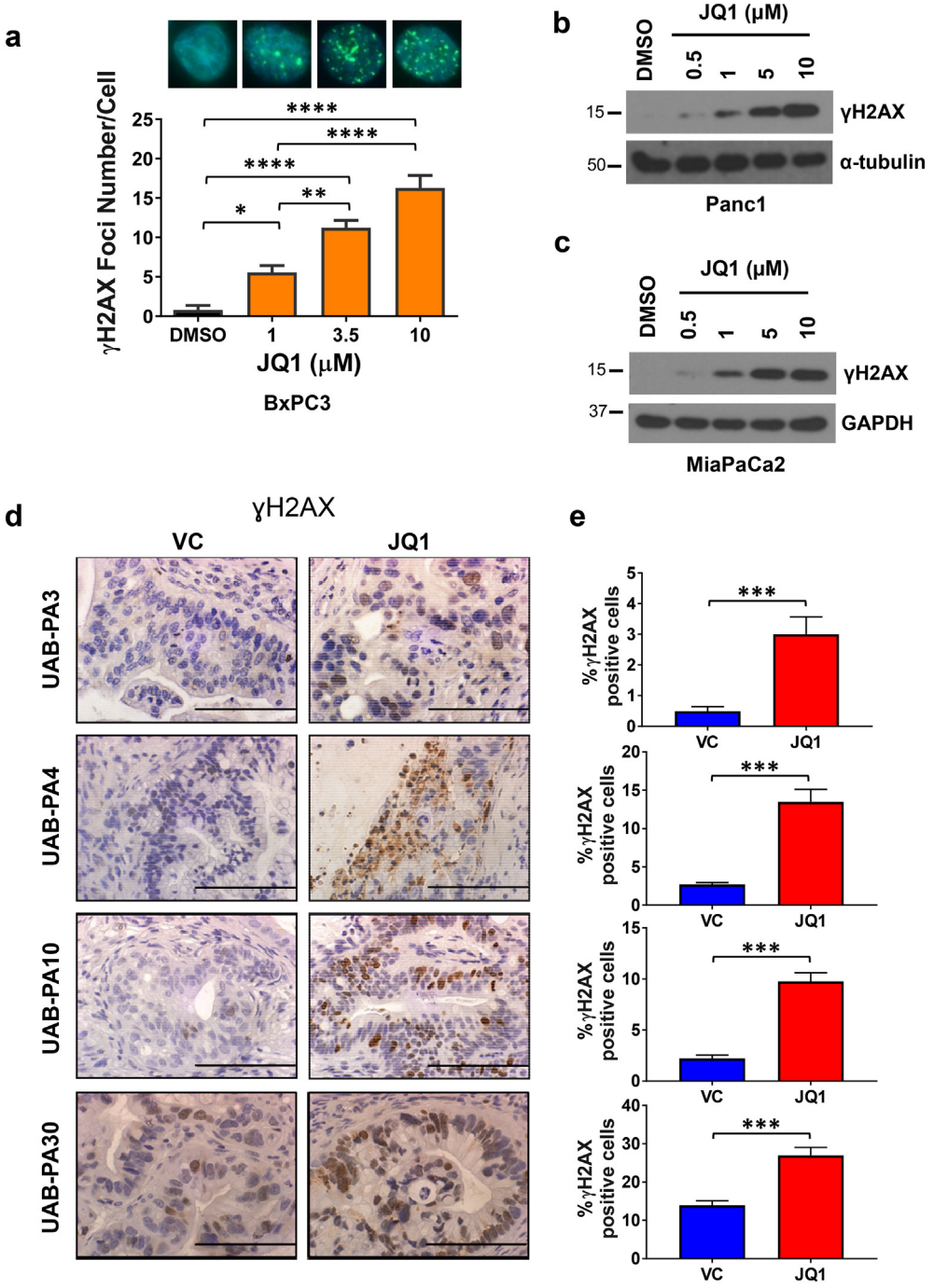

Fig. 1. JQ1 increased the level of DNA damage marker γH2AX *in vitro* and *in vivo*. (a) BxPC3 cells were exposed to JQ1 (0, 1, 3.5, or 10 μM) for 24 h, fixed and immunostained for the DNA damage marker γH2AX, and analyzed for the number of γH2AX-positive fluorescent foci in two independent experiments. Data are presented as mean ± S.E.M and analyzed using a one-way ANOVA (*$p < .05$, **$p < .01$, and ****$p < .0001$). Panc1 (b) or MiaPaCa2 (c) cells were exposed to JQ1 (0.5, 1, 5, or 10 μM) for 48 h, and immunoblotted for γH2AX. (d) Immunohistochemistry analysis for γH2AX of formalin-fixed paraffin-embedded (FFPE) tissues from tumors harvested 24 h after termination of JQ1 treatment of mice bearing UAB-PA3, -PA4, -PA10, and –PA30 tumors. VC = vehicle control. Scale bar = 10 μm. (e) Quantitation of γH2AX immunostaining of tumors exposed to JQ1 *in vivo*. γH2AX levels are shown as the percent of cells positive for γH2AX in 20 random areas. Data are presented as the mean ± S.E.M and a Student's *t*-test was performed (***$p < .001$).

Double-strand break repair is accomplished by non-homologous end joining (NHEJ) and homologous recombination (HR) pathways [21]. Among DNA repair proteins involved in NHEJ and HR pathways, Ku80 and RAD51 are reported to be overexpressed in several tumor types including pancreatic cancer [22–25]. In addition, data from the web-portal UALCAN indicates that patients having tumors that express relatively high levels of Ku80 and RAD51 have a shorter duration of survival [26]. We first characterized expression of Ku80 and RAD51 in the primary tumors from which two models used in this study were derived: UAB-PA4 and UAB-PA16. Consistent with reports in the literature, each primary PDAC tumor expressed higher levels of the NHEJ protein Ku80 (2.6- to 3.4-fold) and HR protein RAD51 (1.7- to 1.8-fold) than normal pancreas (Fig. 2a) [22–25]. We then assessed the impact of JQ1 on expression of Ku80 and RAD51 in PDAC cell lines and in preclinical models derived from these two tumors.

qRT-PCR data demonstrate that a 48h exposure *in vitro* to JQ1 decreased mRNA levels of Ku80 and RAD51 by 40–78% in BxPC3 and Panc1 cells, compared to DMSO controls ($p < .05$, $p < .01$, two-way ANOVA) (Fig. 2b). Immunoblot (IB) analyses corroborate qRT-PCR

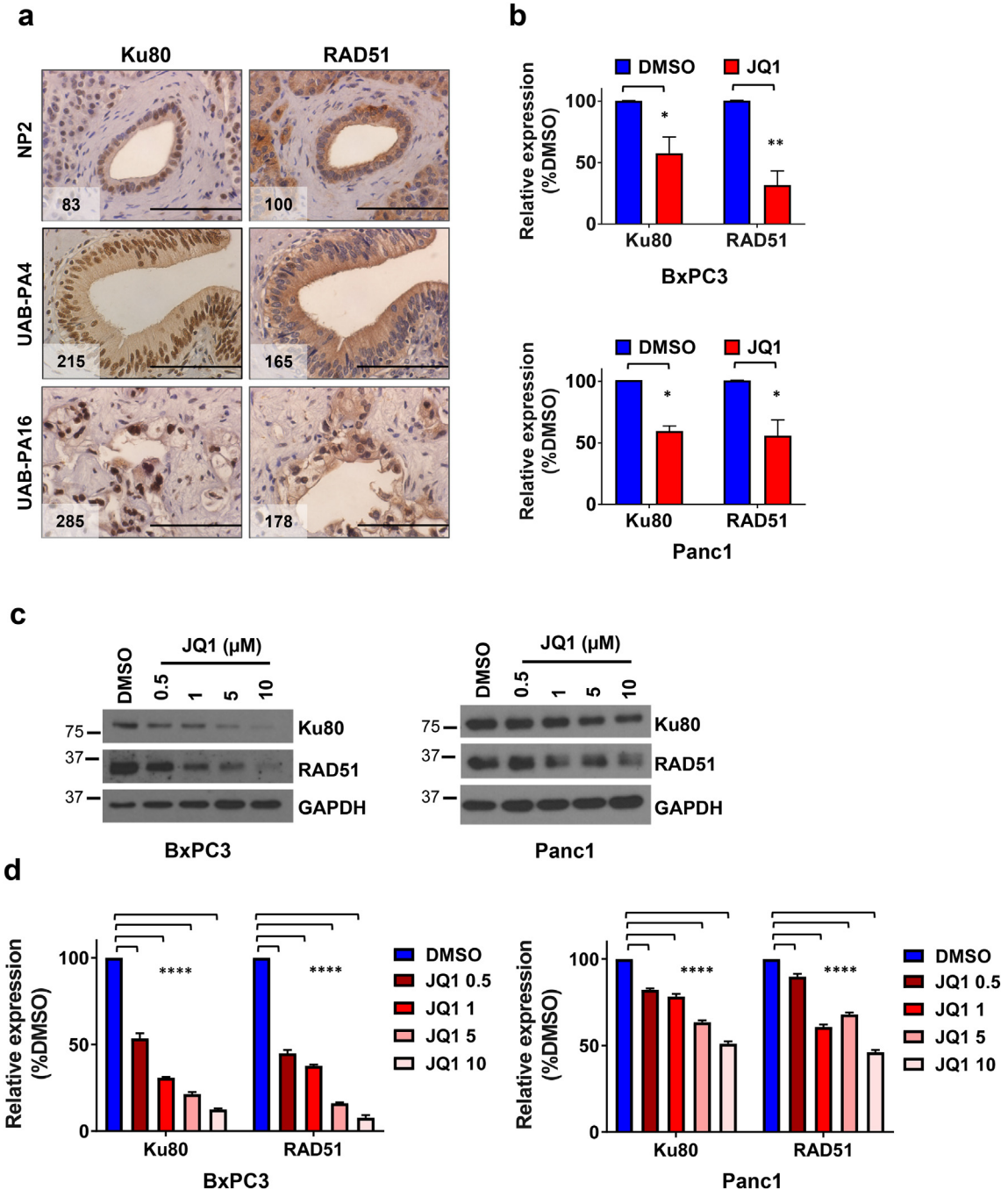

Fig. 2. JQ1 decreased the expression of Ku80 and RAD51. (a) Immunohistochemistry (IHC) was done to detect the expression of Ku80 or RAD51 protein in normal pancreas or primary PDAC tumors. Primary PDAC tumors, UAB-PA4 and UAB-PA16, expressed higher levels of the NHEJ protein Ku80 and HR protein RAD51 compared to a normal pancreas (NP2). Quantitation of IHC results is shown as expression indices (were calculated as described in Materials and Methods) in the lower left-hand corner of each photomicrograph. Scale bar = 10 μM. (b) Forty-eight hour treatment of JQ1 (10 μM) decreased mRNA levels of both Ku80 and RAD51 in BxPC3 or Panc1 PDAC cells using qRT-PCR assays. The sequences for primers used are in Table S1 (Supplementary Materials). Data is shown as the mean ± S.E.M. Two-way analysis of variance (ANOVA) was performed ($^{*}p < .05$, $^{**}p < .01$) using Prism. (c) Immunoblot demonstrating that JQ1 (0.5, 1, 5, or 10 μM) decreased protein expression of Ku80 and RAD51 in BxPC3 or Panc1 PDAC cells treated for 48 h. (d) The immunoblot data in c were quantitated as percent DMSO using ImageStudio Lite (LI-COR Biosciences) and are reported as bar graphs mean ± S.D. Analysis was done by two-way ANOVA ($^{****}p < .0001$).

data and demonstrate that JQ1 reduced Ku80 and RAD51 protein levels in these cell lines (Fig. 2c), in a dose-dependent manner (Fig. 2d).

3.3. JQ1 + olaparib suppressed tumor growth in patient-derived xenograft (PDX) models of PDAC in vivo

Our data show that JQ1 increases the level of γH2AX and decreases expression of DNA repair proteins Ku80 and RAD51 (Figs.1, 2). PARP inhibitors (PARPi) are selectively cytotoxic to cells deficient in double-strand DNA repair or to cells treated with DNA damaging agents [27,28]. We hypothesized that JQ1 would sensitize PDAC cells to PARPi and that JQ1 + the PARPi olaparib would have a greater than additive anti-proliferative effect. Olaparib has efficacy as a single agent and is approved for use in BRCA mutated ovarian cancer [29,30].

We first evaluated the efficacy of JQ1 + olaparib in PDAC PDX models UAB-PA4 and UAB-PA16. Both models harbor a G12D mutation in codon 12 of the *KRAS* gene, as is common in primary PDAC tumors. The TNM (tumor, nodes, metastasis) classification was pT3N0 and

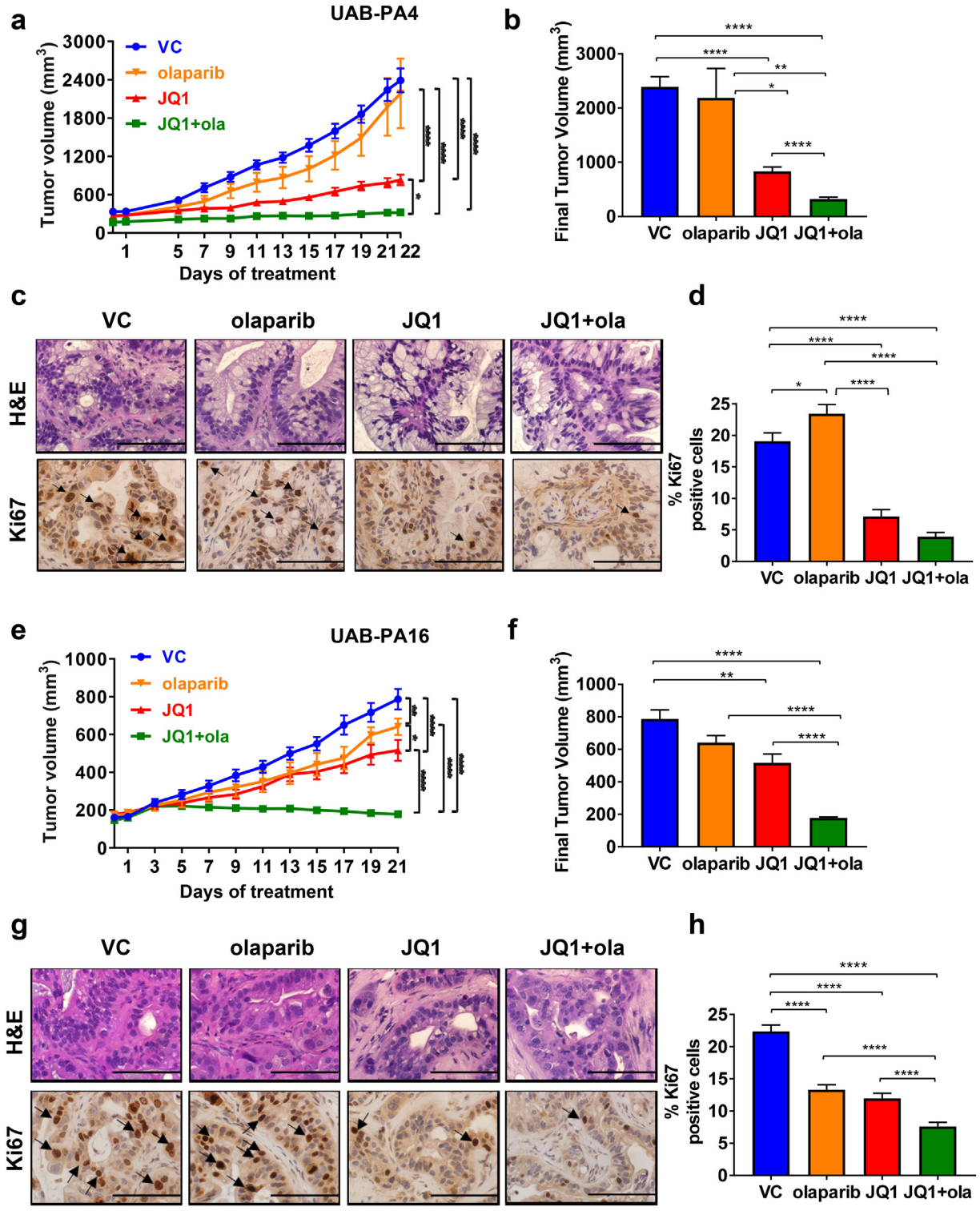

Fig. 3. JQ1 + olaparib suppressed tumor growth, and decreased the expression of proliferation marker Ki67 in both UAB-PA4 and -PA16 patient-derived xenograft models of PDAC. Mice bearing bilateral tumors ~100-200 mm^3 in size were randomized to four groups of 5 mice/group (except VC for UAB-PA4 [$n = 4$]). Mice were treated with vehicle control (VC), JQ1 (50 mg/kg), olaparib (50 mg/kg) or JQ1 (50 mg/kg) + olaparib (50 mg/kg) daily for 21 days. Data for UAB-PA4 tumors represent average tumor volume ± S.E.M. for 8 (VC, olaparib) or 10 (JQ1, JQ1 + olaparib) tumors/group. Data for UAB-PA16 tumors represent average ± S.E.M. for 9 (VC, olaparib) or 10 (JQ1, JQ1 + olaparib) tumors/group. We excluded tumors that did not grow. Average tumor volume (a, e; all values are presented as mean ± S.E.M.) for UAB-PA4 or -PA16 were calculated as described in Materials and Methods. Two-way ANOVA was performed (*$p < .05$, **$p < .01$, ****$p < .0001$). (b, f) Final tumor volume was analyzed by Student's t-test (*$p < .05$, **$p < .01$, ***$p < .001$, ****$p < .0001$). (c, g) Tumor tissue was harvested 24 h after completion of treatment, H&E staining done to visualize morphology, and immunostaining done to detect the proliferation marker Ki67. Scale bar = 10 μm. (d, h) IHC data for Ki67 were quantitated as the number of Ki67 positive tumor cells divided by total number of tumor cells and are reported as bar graphs mean ± S.E.M and analyzed using one-way ANOVA (*$p < .05$, ****$p < .0001$).

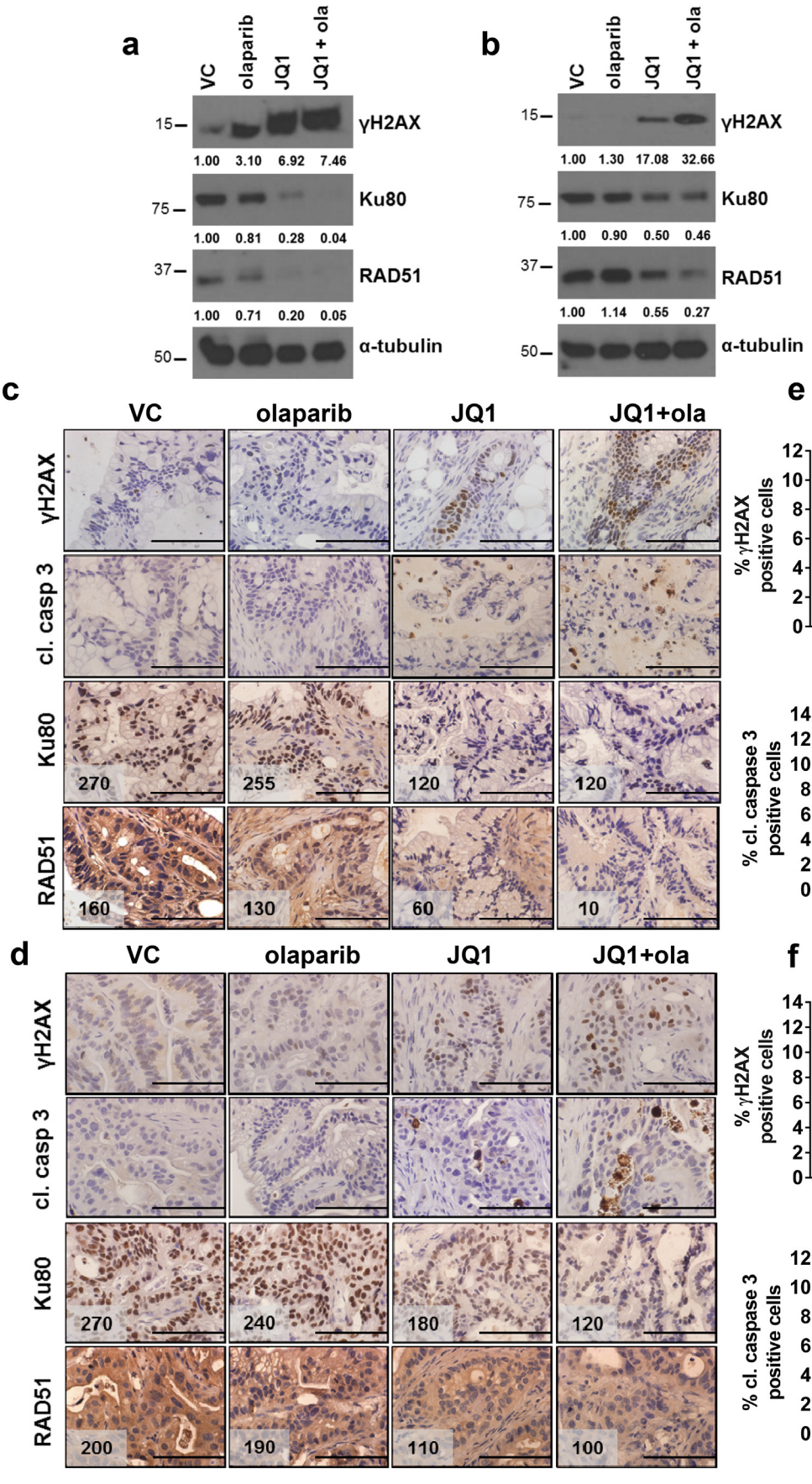
a
VC
olaparib
JQ1
JQ1 + ola
15
γH2AX
1.00 3.10 6.92 7.46
75
Ku80
1.00 0.81 0.28 0.04
37
RAD51
1.00 0.71 0.20 0.05
50
α-tubulin
b
VC
olaparib
JQ1
JQ1 + ola
15
γH2AX
1.00 1.30 17.08 32.66
75
Ku80
1.00 0.90 0.50 0.46
37
RAD51
1.00 1.14 0.55 0.27
50
α-tubulin
c
VC
olaparib
JQ1
JQ1+ola
γH2AX
cl. casp 3
Ku80
270
255
120
120
RAD51
160
130
60
10
e
% γH2AX positive cells
VC olaparib JQ1 JQ1+ola
% cl. caspase 3 positive cells
VC olaparib JQ1 JQ1 + ola
d
VC
olaparib
JQ1
JQ1+ola
γH2AX
cl. casp 3
Ku80
270
240
180
120
RAD51
200
190
110
100
f
% γH2AX positive cells
VC olaparib JQ1 JQ1+ola
% cl. caspase 3 positive cells
VC olaparib JQ1 JQ1 + ola

pT2N1 for UAB-PA4 and UAB-PA16, respectively. Both tumors were derived from grade 3 poorly differentiated stage II PDAC tumors [7,18]. JQ1 (50 mg/kg) and/or olaparib (50 mg/kg) were administered daily for 21 days to mice bearing UAB-PA4 or -PA16 tumors. Olaparib as a single agent inhibited growth of UAB-PA16 tumors ($p < .01$, two-way ANOVA) but did not inhibit growth of UAB-PA4 tumors (Fig. 3a, e). JQ1 as a single agent suppressed tumor growth in both models, compared to vehicle control ($p < .0001$, two-way ANOVA). The combination of JQ1 + olaparib was more effective than either drug alone in both UAB-PA4 (Fig. 3a, b) and -PA16 (Fig. 3e, f) PDX models. All mice in all treatment groups had consistent body weights (Fig. S1). Tumors were harvested at completion of therapy and archived for immunostaining and immunoblot analyses.

The observed inhibition of tumor growth was consistent with immunostaining data for the proliferation marker Ki67 (Fig. 3c, g). Ki67 levels in UAB-PA4 and -PA16 tumors exposed to JQ1 were lower than in tumors exposed to vehicle control (VC) ($p < .0001$, one-way ANOVA) (Fig. 3d, h). JQ1 + olaparib decreased Ki67 expression more than JQ1 or olaparib alone in both models. The data are consistent with tumor volume data and indicate that the combination was more effective than either drug as a single agent in inhibiting tumor cell proliferation *in vivo*.

3.4. JQ1 + olaparib decreased expression of DNA repair proteins Ku80 and RAD51 in vivo

Tumor tissue harvested at completion of efficacy studies were then immunoblotted (IB) or immunostained (IHC) to assess the effect of JQ1 ± olaparib on γH2AX, Ku80, and RAD51. IB data supported previous data showing that JQ1 increased levels of the DNA damage marker γH2AX 7- to 17-fold, and that JQ1 + olaparib increased γH2AX by 7.5- to 33-fold compared to vehicle controls (VC) in both PDX models (Fig. 4a, b). IHC data also show that exposure to JQ1 or JQ1 + olaparib *in vivo* increased the percent of γH2AX positive cells compared to VC ($p < .05$, one-way ANOVA) or to olaparib ($p < .001$, one-way ANOVA), and increased the apoptosis marker cleaved caspase 3 compared to VC or olaparib alone ($p < .01$, one-way ANOVA) (Fig. 4c-4f). Further, IB data demonstrated that JQ1 decreased expression of the NHEJ repair protein Ku80 and the HR DNA repair protein RAD51 by ~45–80%, and the combination of JQ1 + olaparib decreased *in vivo* expression of both proteins by up to ~95% in UAB-PA4 and -PA16 tumor models (Fig. 4a, 4b). IHC data corroborated these IB data (Fig. 4c-4f). The data suggest that decreased levels of DNA double-strand break repair proteins Ku80 and RAD51 lead to accumulation of DNA damage and increased apoptotic index, as reflected by the increase in cleaved caspase 3 (Fig. 4).

3.5. Combinations of JQ1 + PARPi exerted synergistic cytotoxicity in PDAC cell lines

The observed efficacy of JQ1 + olaparib in PDAC PDX models were consistent with the original hypothesis that JQ1-induced accumulation of DNA damage would augment the anti-proliferative effects of PARPi. To address potential mechanistic aspects of the complementary activity of these two agents, we first confirmed that similar augmentation of efficacy was evident using *in vitro* models. We exposed BxPC3 or Panc1 PDAC cells to a range of concentrations of JQ1 (0.1-100 μM) + the indicated fixed concentration of PARPi for 72 h and assessed cell viability by alamarBlue assay. In the presence of the PARPi veliparib, the IC_{50} of JQ1 decreased by ~18-fold in BxPC3 (Fig. 5a). Similarly, the PARPi olaparib decreased the IC_{50} of JQ1 by ~6-fold in Panc1 cells (Fig. 5b). IF data were also consistent with *in vivo* data, exposure of BxPC3 cells to a fixed ratio of JQ1 3.5 μM + veliparib10μM for 24 h increased levels of the DNA damage marker γH2AX, compared to JQ1 alone ($p < .01$, one-way ANOVA) (Fig. 5c). Further, we assessed the effect of JQ1 + olaparib (1:1 ratio) on colony formation, using Panc1 cells (Fig. 5d). Panc1 cells were exposed to drug(s) for 72 h, incubated for an additional 11 days in the absence of drug, and colonies counted on day 14. Notably, the anti-proliferative effect of the combination remained evident after a week in drug-free medium ($p < .01$, one-way ANOVA). These results suggest that it may be useful to compare the efficacy JQ1 + olaparib given on an intermittent schedule, rather than basing *in vivo* schedules of administration predominantly on the relatively short half-life ($t_{1/2}$) of JQ1.

To facilitate calculation of combination indices (CI), we exposed BxPC3 and Panc1 cell lines to a fixed ratio (1:1) of JQ1 + veliparib or olaparib for 72 h and assessed cell viability with alamarBlue assays. CI values demonstrate that both combinations were synergistic in BxPC3 and Panc1 cell lines (Fig. 5e).

As above, both synergistic combinations were associated with an increase in γH2AX level in BxPC3 cells (Fig. 5c, f). Further, JQ1 decreased Ku80 and RAD51 expression and JQ1 + PARPi augmented this down-regulation. JQ1 + olaparib also increased p21 (CDKN1A) expression which is induced by DNA damage (Fig. 5f) [31]. Comparable data were obtained with Panc1 and MiaPaCa2 cells (Fig. S2).

3.6. JQ1 prevented formation of RAD51 foci in BxPC3 cells

Recruitment of RAD51 to sites of DNA damage is a critical step in HR repair, with increases in RAD51 foci formation reflecting levels of HR DNA double-strand break repair. To assess the effect of JQ1 on HR repair in cells, we exposed BxPC3 cells to 20 μM JQ1 for 24 h to increase DNA damage, and detect RAD51 foci using FITC-labeled anti-RAD51 (Fig. 5g). HR competent cells would be predicted to have more detectable foci, as RAD51 would be recruited to sites undergoing repair. As expected, JQ1 decreased RAD51 foci formation in BxPC3 cells ($p < .01$, Student's *t*-test). Olaparib was used as a positive control since inhibition of PARP1 causes replication-associated DNA double-strand breaks which are predominantly repaired by the HR pathway [12,13,32].

3.7. Expression of Ku80 and RAD51 was BET-dependent

JQ1 associates with 96% of genetic loci to which BRD2 binds and with 99% of loci to which BRD4 binds, indicating that JQ1 targets BRD2 and BRD4 [33]. Current literature suggests that BRD4-associated mechanisms regulate expression of unique subsets of genes in different cell types. Specific gene products that depend on BRD4 or BRD2 for expression in pancreatic cancer cells have not been investigated. Data above suggest that in PDAC cells, BRD4 or BRD2 regulate expression of Ku80 and RAD51 and, conversely, that inhibition of either of these BET proteins decreases Ku80 and RAD51 expression. We addressed this hypothesis directly using chromatin immunoprecipitation (ChIP) assays to assess the occupancy of BRD4 and BRD2 on the promoter sequences of Ku80 and RAD51 in the presence and absence of JQ1 (Fig. 6a, b). The data demonstrate that JQ1 decreased the association of BRD4 with promoters of Ku80 and RAD51 by ~40% and ~63%, respectively, compared to DMSO controls, in BxPC3 cells (Fig. 6a), and decreased the association of

Fig. 4. JQ1 + olaparib increased the levels of DNA damage marker γH2AX and reduced the expression of Ku80 and RAD51 in *in vivo* models of PDAC. Immunoblots (IB) were done to detect γH2AX and DNA repair proteins, Ku80 and RAD51 using UAB-PA4 (a) or UAB-PA16 (b) tumors harvested from mice 24 h following final treatment (see Materials and Methods). Quantitation by densitometry of results is shown below each IB image. Immunohistochemistry was done to detect γH2AX, apoptosis marker cleaved caspase 3 (cl. casp 3) and DNA repair proteins, Ku80 and RAD51 using UAB-PA4 (c) or UAB-PA16 (d) thin sections of tumors harvested from mice 24 h following final treatment. Scale bar = 10 μM. Quantitation of results is shown either as a bar graph for γH2AX and cleaved caspase 3 (cl. casp 3) (e, f for UAB-PA4 and UAB-PA16, respectively) or as expression indices (were calculated as described in Materials and Methods) in the lower left-hand corner of each photomicrograph depicting IHC image. Data are presented as mean ± S.E.M. and analyzed with one-way ANOVA (*$p < .05$, **$p < .01$, ***$p < .001$, ****$p < .0001$).

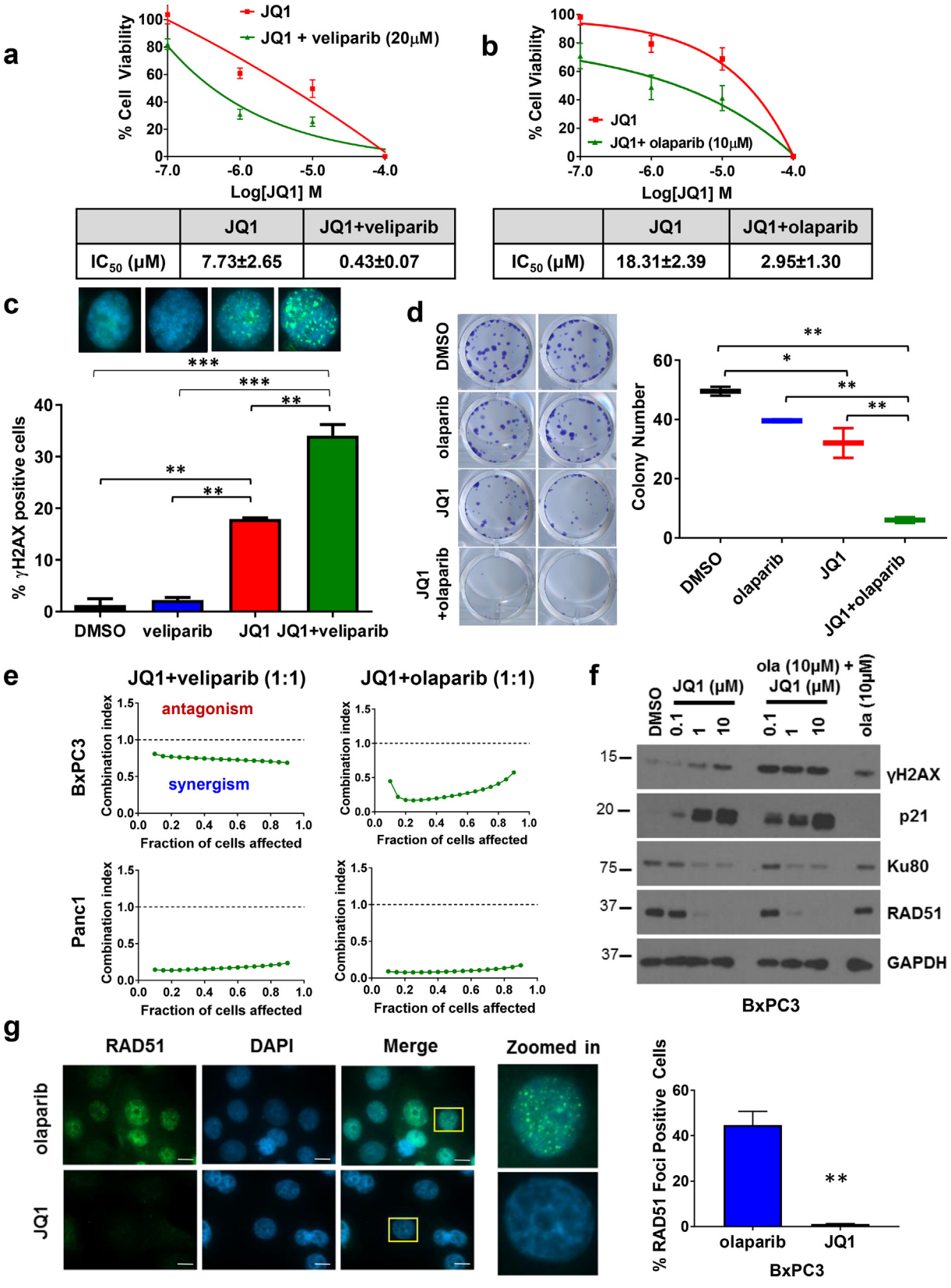

	JQ1	JQ1+veliparib
IC_{50} (μM)	7.73±2.65	0.43±0.07

	JQ1	JQ1+olaparib
IC_{50} (μM)	18.31±2.39	2.95±1.30

BRD2 with promoters of Ku80 and RAD51 by ~48% and ~55%, respectively in Panc1 cells (Fig. 6b).

To corroborate these data indicating that expression of these DNA repair enzymes Ku80 and RAD51 was BRD4- or BRD2-dependent in PDAC cells, we down-regulated BRD4 or BRD2 expression using two different short hairpin RNAs (shBRD4–1, shBRD4–2, shBRD2–1, shBRD2–2) and evaluated the effect of the direct decrease in BRD4 or BRD2 expression on Ku80 and RAD51 proteins. As shown in Fig. 6c, when the shBRD4–1 construct downregulated BRD4 expression by 53%, the level of Ku80 protein was decreased by 35% and RAD51 by 93% in BxPC3 cells. When BRD2 is down-regulated by 82% in Panc1 cells, the expression of Ku80 and RAD51 was decreased by 69% and

93% respectively (Fig. 6d). Similar results were obtained with the second set of shRNA's (Fig. S3). The data were consistent with ChIP data, and we concluded that in PDAC cells, Ku80 and RAD51 expression was BRD4- and BRD2-dependent.

The data demonstrate that translational repression of BRD4 or BRD2 by shRNA and pharmacological inhibition of BET protein activity by JQ1 decreased expression of DNA repair proteins Ku80 and RAD51 in PDAC cells. The data suggest that this inhibition may contribute to the synergy of JQ1 + PARPi in this tumor cell type.

In summary, JQ1 decreased expression of DNA repair proteins Ku80 and RAD51, induced apoptosis, facilitated an increase in levels of DNA damage, exerted synergistic cytotoxicity *in vitro* when combined with the PARPi veliparib or olaparib, and suppressed tumor growth in two PDX models of PDAC. Mechanistic data suggest that inhibition of BET-dependent expression of the HR DNA repair protein RAD51 and the NHEJ repair protein Ku80 contributes to the observed efficacy and synergy of JQ1 + olaparib.

4. Discussion

This study evaluated the anti-proliferative activity of the BET inhibitor JQ1 in combination with a PARP inhibitor (veliparib or olaparib) in PDAC cell lines *in vitro* and of JQ1 + olaparib in independently derived PDX models *in vivo*. It also examined the effect of JQ1 as a single agent or in combination on levels of DNA damage and on expression of DNA repair proteins Ku80 and RAD51. The study addressed the hypothesis that inhibition of the BET proteins BRD4 or BRD2 attenuates DNA double-strand repair by reducing Ku80 and RAD51 expression, therefore augmenting the anti-proliferative activity of JQ1 in this tumor type. *In vitro* and *in vivo* data supported this hypothesis. The data show that JQ1 + olaparib is synergistic *in vitro* and has greater efficacy than either drug alone *in vivo*. The data also demonstrate that expression of DNA repair proteins Ku80 and RAD51 is regulated by BRD4 and BRD2 in PDAC cells.

Unlike potencies in the nanomolar range that have been reported for cell lines derived from hematological malignancies [34–36], JQ1 as a single agent exhibits IC_{50}s *in vitro* in the micromolar range for BxPC3 and Panc1 pancreatic cancer cell lines. However, efficacious regimens of JQ1 *in vivo* are comparable to those reported for preclinical models of leukemic and other solid malignancies. A similar discrepancy between *in vitro* potency and *in vivo* utility has been documented for other agents such as vorinostat (SAHA) and erlotinib [37–42], and likely reflects differences in factors such as duration of exposure to drug *in vitro* (Fig. S4) and, most importantly, the therapeutic index of each agent. Notably, *in vivo* data in this report indicate a favorable therapeutic index for JQ1. The efficacy for BET inhibitors such as JQ1, however, may differ with tumor type. Recent literature suggests that BET proteins associate with specific subsets of promoters or super enhancers in a tumor type-specific manner. Loven, et al. demonstrated that expression of super enhancer-associated genes c-Myc, IRF4, PRDM1/BLIMP-1 and XBP1 that actively contribute to multiple myeloma progression, decreased when BET function was inhibited [43]. In contrast, Lenhart *et al* reported that JQ1 did not inhibit c-Myc protein expression in small cell lung cancer cell lines, but did inhibit expression of the transcription factor achaete-scute homolog-1 (ASCL1) [44]. Identification of BET inhibitors that regulate expression of genes known to promote growth of specific types of tumors might maximize therapeutic indices and the utility of each BET inhibitor.

Recent literature also documents encouraging results for the potential utility of BET inhibitors in combination with agents having complementary mechanisms of cytotoxicity. A noteworthy study demonstrated that in small cell lung cancer cells the combination of the BET inhibitor ABBV-075 and the BCL2 inhibitor venetoclax (ABT-199) induced apoptosis, as assessed by an increase in expression of the pro-apoptotic protein BIM and a decrease in anti-apoptotic proteins BCL-2 and BCL-xL. This combination showed strong synergy *in vitro* and tumor regressions *in vivo* [45]. A second study showed that combining JQ1 with the histone deacetylase (HDAC) inhibitor vorinostat (SAHA) improved overall survival in *KRAS:p53* mutant mice which develop pancreatic tumors with high penetrance [8]. A third study by Yang, *et al* documented that JQ1 sensitized HR proficient ovarian and breast carcinoma tumor models to olaparib [46]. That study also demonstrated that JQ1 decreased expression of HR-associated repair proteins BRCA1 and RAD51 in cells exposed to JQ1 *in vitro*. Our results extend observations of Yang *et al* in that in PDAC cells JQ1 suppressed expression of a protein associated with NHEJ repair (Ku80) as well as a protein associated with HR repair (RAD51). If, as Yang, *et al* suggested, there is a compensatory upregulation of NHEJ when HR is inhibited, simultaneous inhibition of both processes might be therapeutically beneficial. Differences between the study of Yang, *et al* and the data presented herein suggest that JQ1 may affect different genes in different cell types. Further, it is becoming evident that specific PARPi as single agents or in combination have unique characteristics with respect to efficacy [47]. For example, the DNA damaging agent temozolomide + olaparib was superior to temozolomide + veliparib, even though olaparib and veliparib had comparable potency as single agents *in vitro* in DT40 gallus bursa lymphoma cells [47]. Neither PARPi was effective in PARP1-deficient cells and each inhibitor synergized with temozolomide, although synergy was evident at lower concentrations of olaparib compared to veliparib. With the HR proficient PDAC cells in our study (BxPC3, Panc1), effects of veliparib and olaparib were comparable when combined with JQ1.

Data in this manuscript document the novel observations that the combination of a BET inhibitor and a PARP inhibitor exerts synergistic cytotoxicity *in vitro* and suppresses tumor growth greater than either agent alone *in vivo*, in PDAC models including two independently derived PDX models. Mechanistically, the data indicate that the observed synergy and efficacy likely depends on simultaneous inhibition of BRD4- and BRD2-dependent expression of HR DNA repair protein

Fig. 5. Simultaneous exposure of JQ1 + PARPi increased DNA damage, reduced expression of DNA repair proteins Ku80 and RAD51, inhibited colony formation, and induced synergistic cytotoxicity in PDAC cells. BxPC3 (a) or Panc1 (b) cells were exposed to the indicated concentrations of JQ1 (0.1-100 μM) in combination with 20 μM veliparib or 10 μM olaparib for 72 h, after which alamarBlue solution was added and fluorescence read. Data were normalized to controls at each time point, with control values = 100%. Each point represents the average of quadruplicate wells from three independent assays. Data are presented as mean ± S.D. IC_{50} values of JQ1 as a single agent or in combination with veliparib or olaparib are shown in a table below the graph. (c) JQ1 + veliparib increased DNA damage, as reflected by an increase in γH2AX positive BxPC3 cells. The percent of γH2AX-positive cells following exposure to DMSO, veliparib (10 μM), JQ1 (3.5 μM), or JQ1 (3.5 μM) + veliparib (10 μM) for 24 h were quantitated. The % of γH2AX positive cells was calculated by counting the number of positive cells (cells containing ≥5 foci) and dividing it by the total number of cells in two independent experiments (a minimum of 200 cells were counted per experiment). A representative IF stain is shown for each treatment group. Data presented as mean ± S.E.M. and analyzed by one-way ANOVA (**$p < .01$, ***$p < .001$). (d) Panc1 cells were exposed to DMSO, JQ1 (1 μM), olaparib (1 μM) or the combination (1:1) for 72 h, at which time drug-containing medium was replaced with drug-free medium and the cells were cultured for an additional 11 days. On day 14, cells were fixed and stained with crystal violet, and quantitation of viable colonies done by determining number of colonies having >50 cells. The data are shown as a box and whisker plot with the whiskers showing the min and max. Analysis was done using a one-way ANOVA (*$p < .05$, **$p < .01$). (e) JQ1 + PARPi are synergistic in PDAC cells. BxPC3 and Panc1 cells were exposed to JQ1 + veliparib (1:1) (0.1-25 μM) or JQ1 + olaparib (1:1) (0.1-100 μM) for 72 h, and cell viability analyzed by alamarBlue assay. Combination indices (CI) are plotted to fraction of cells affected (Fa) using CompuSyn software which was based on the Chou-Talalay method. A CI of <1.0 indicates synergism. (f) JQ1 and JQ1 + olaparib increased the levels of γH2AX and p21, and decreased the expression of Ku80 and RAD51 in BxPC3 cells. BxPC3 cells were exposed to the indicated concentrations of JQ1 (0.1, 1, and 10 μM) with or without 10 μM olaparib for 48 h, and cell lysates were immunostained for the indicated proteins. (g) RAD51 nuclear foci formation assays were done with BxPC3 cells using JQ1 or olaparib as a control. Cells were exposed to JQ1 (20 μM) or olaparib (1 μM) for 24 h, fixed and stained with FITC-RAD51 antibody. DAPI was used to detect nuclei. Quantitation was done by counting the percent (%) RAD51 foci positive cells and plotted as mean ± S.E.M. The % of RAD51 positive cells was calculated by counting the number of positive cells (cells containing ≥5 foci) and dividing it by the total number of cells in three independent experiments (a minimum of 50 cells were counted per experiment). Student's *t*-test was performed (**$p < .01$, Scale bar = 10 μm).

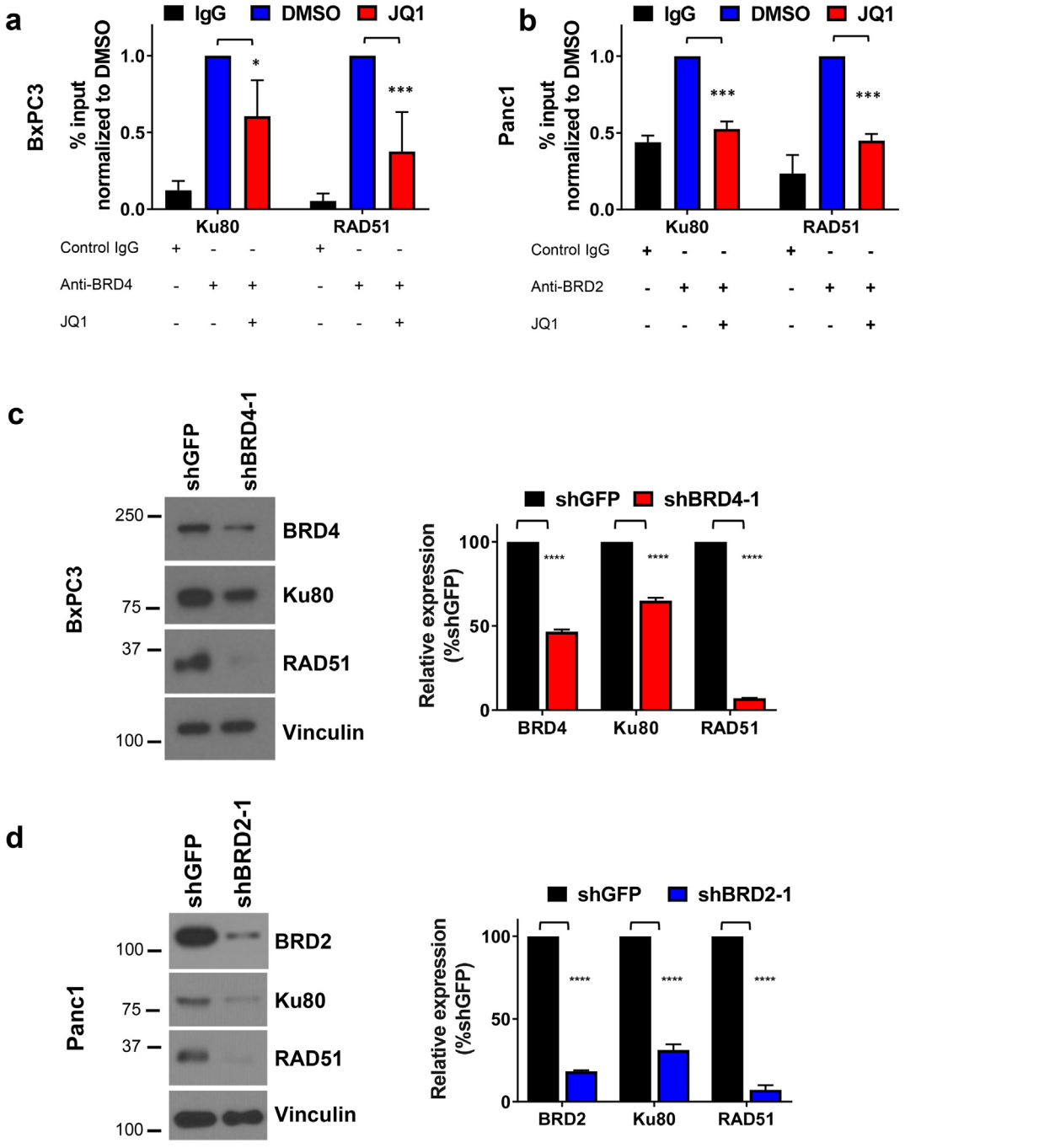

Fig. 6. Expression of Ku80 and RAD51 was BET-dependent. Chromatin immunoprecipitation assays of BRD4 in BxPC3 cells (a) or BRD2 in Panc1 cells (b) on the promoter sequences of Ku80 and RAD51. Forty-eight hour exposure to JQ1 (10 μM) decreased the association of BRD4 or BRD2 with the promoter sequences of Ku80 and RAD51 compared to the vehicle (DMSO) controls. Rabbit IgG was used as a negative control. The data is shown as the mean ± S.D. and two-way ANOVA was used to identify differences in levels of expression ($^{*}p < .05$, $^{***}p < .001$). Experiments in which shRNA was used to decrease expression of BRD4 in BxPC3 (c) or BRD2 (d) in Panc1 cells using shRNA (see Table S1 for sequences), decreased the expression of both Ku80 and RAD51. Quantitation of 6c and 6d is shown in the right panel as the mean ± S.D. in the bar graph. Two-way ANOVA was used to determine significance ($^{****}p < .0001$). shGFP serves as a control.

RAD51 and NHEJ repair protein Ku80 to confer DNA double-strand break repair deficiency in this tumor cell type. Work is ongoing to determine if *in vitro* mechanistic findings with BxPC3 and Panc1 cells are consistent among additional PDAC cell lines that express wild type compared to mutant *KRAS* and among PDX tumors of independent origin. We propose that a DNA repair deficient phenotype induced by JQ1 sensitized tumors to the PARP inhibitor olaparib. The work provides mechanistic and efficacy data to support assessing combinations of BET and PARP inhibitors in treating patients with PDAC.

Funding Sources and Acknowledgements

This study was supported by the National Institutes of Health (National Cancer Institute) grants R01CA208272 and R21CA205501 (K.J.Y.). A.L.M. is a recipient of the predoctoral training fellowship in Cell and Molecular Biology (CMB) T32 training grant (2017–2018). R.C.A.M.vW. is supported by DoD OCRP pilot grant W81XWH-15-1-0198. E.S·Y is supported by AstraZeneca, ASCO, Eli Lilly, Novartis and PUMA. The funding sources had no role in the study design, data

collection, analysis and interpretation, and writing of the manuscript. The corresponding author had full access to all the data in the study and had final responsibility for the decision to submit for publication.

Conflicts of interest (declaration of interests)

K.J.Y receives grants from the National Institutes of Health (R01CA208272 and R21CA205501). A.L.M. received the predoctoral training fellowship in CMB T32 training grant (2017–2018). R.C.A.M.vW received DoD OCRP pilot grant (W81XWH-15-1-0198). E.S.Y. receives personal fee from AstraZeneca and receives funding from ASCO, Eli Lilly, Novartis, and PUMA. J.E.B is now an executive and shareholder of Novartis AG, and has been a founder and shareholder of SHAPE (acquired by Medivir), Acetylon (acquired by Celgene), Tensha (acquired by Roche), Syros, Regency and C4 Therapeutics. J.E.B. has a patent US 8,981,083 B2 to Roche-Genetech. All other authors declare no conflicts of interest.

Author contributions

A.L.M. designed and performed experiments (*in vitro* and *in vivo*), analyzed data, and wrote the manuscript, S.C.F., T.L.G. performed *in vivo* experiments, P.L.G. performed *in vitro* experiments, L.N.C. interpreted data (histology of primary PDAC tissue), E.S.Y., J.E.B. conceived study, provided critical reagents, and interpreted data. R.C.A.M. vW. conceived study, interpreted data, and wrote the manuscript. K.J.Y. conceived, designed and supervised study, interpreted data, and wrote the manuscript. All authors approved the final manuscript.

Appendix A. Supplementary data

Supplementary data to this article can be found online at https://doi.org/10.1016/j.ebiom.2019.05.035.

References

[1] Siegel RL, Miller KD, Jemal A. Cancer statistics, 2017. CA Cancer J Clin 2017;67(1):7–30.
[2] Conroy T, Desseigne F, Ychou M, et al. FOLFIRINOX versus gemcitabine for metastatic pancreatic cancer. N Engl J Med 2011;364(19):1817–25.
[3] Shi J, Vakoc CR. The mechanisms behind the therapeutic activity of BET bromodomain inhibition. Mol Cell 2014;54(5):728–36.
[4] Huang Y, Nahar S, Nakagawa A, et al. Regulation of GLI underlies a role for BET bromodomains in pancreatic Cancer growth and the tumor microenvironment. Clin Cancer Res 2016;22(16):4259–70.
[5] Wang YH, Sui YN, Yan K, Wang LS, Wang F, Zhou JH. BRD4 promotes pancreatic ductal adenocarcinoma cell proliferation and enhances gemcitabine resistance. Oncol Rep 2015;33(4):1699–706.
[6] Sahai V, Kumar K, Knab LM, et al. BET bromodomain inhibitors block growth of pancreatic cancer cells in three-dimensional collagen. Mol Cancer Ther 2014;13(7):1907–17.
[7] Garcia PL, Miller AL, Kreitzburg KM, et al. The BET bromodomain inhibitor JQ1 suppresses growth of pancreatic ductal adenocarcinoma in patient-derived xenograft models. Oncogene 2016;35(7):833–45.
[8] Mazur PK, Herner A, Mello SS, et al. Combined inhibition of BET family proteins and histone deacetylases as a potential epigenetics-based therapy for pancreatic ductal adenocarcinoma. Nat Med 2015;21(10):1163–71.
[9] Doroshow DB, Eder JP, LoRusso PM. BET inhibitors: a novel epigenetic approach. Ann Oncol 2017;28(8):1776–87.
[10] Floyd SR, Pacold ME, Huang Q, et al. The bromodomain protein Brd4 insulates chromatin from DNA damage signalling. Nature 2013;498(7453):246–50.
[11] Stanlie A, Yousif AS, Akiyama H, Honjo T, Begum NA. Chromatin reader Brd4 functions in Ig class switching as a repair complex adaptor of nonhomologous end-joining. Mol Cell 2014;55(1):97–110.
[12] Bryant HE, Schultz N, Thomas HD, et al. Specific killing of BRCA2-deficient tumours with inhibitors of poly(ADP-ribose) polymerase. Nature 2005;434(7035):913–7.
[13] Farmer H, McCabe N, Lord CJ, et al. Targeting the DNA repair defect in BRCA mutant cells as a therapeutic strategy. Nature 2005;434(7035):917–21.
[14] Palma JP, Wang YC, Rodriguez LE, et al. ABT-888 confers broad in vivo activity in combination with temozolomide in diverse tumors. Clin Cancer Res 2009;15(23):7277–90.
[15] Plummer R, Jones C, Middleton M, et al. Phase I study of the poly(ADP-ribose) polymerase inhibitor, AG014699, in combination with temozolomide in patients with advanced solid tumors. Clin Cancer Res 2008;14(23):7917–23.
[16] Rottenberg S, Jaspers JE, Kersbergen A, et al. High sensitivity of BRCA1-deficient mammary tumors to the PARP inhibitor AZD2281 alone and in combination with platinum drugs. Proc Natl Acad Sci U S A 2008;105(44):17079–84.
[17] Scott CL, Swisher EM, Kaufmann SH. Poly (ADP-ribose) polymerase inhibitors: recent advances and future development. J Clin Oncol 2015;33(12):1397–406.
[18] Garcia PL, Council LN, Christein JD, et al. Development and histopathological characterization of tumorgraft models of pancreatic ductal adenocarcinoma. PloS One 2013;8(10):e78183.
[19] Muralidharan SV, Bhadury J, Nilsson LM, Green LC, McLure KG, Nilsson JA. BET bromodomain inhibitors synergize with ATR inhibitors to induce DNA damage, apoptosis, senescence-associated secretory pathway and ER stress in Myc-induced lymphoma cells. Oncogene 2016;35(36):4689–97.
[20] Bonner WM, Redon CE, Dickey JS, et al. GammaH2AX and cancer. Nat Rev Cancer 2008;8(12):957–67.
[21] O'Connor MJ. Targeting the DNA damage response in Cancer. Mol Cell 2015;60(4):547–60.
[22] Maacke H, Jost K, Opitz S, et al. DNA repair and recombination factor Rad51 is overexpressed in human pancreatic adenocarcinoma. Oncogene 2000;19(23):2791–5.
[23] Nagathihalli NS, Nagaraju G. RAD51 as a potential biomarker and therapeutic target for pancreatic cancer. Biochim Biophys Acta 2011;1816(2):209–18.
[24] Moeller BJ, Yordy JS, Williams MD, et al. DNA repair biomarker profiling of head and neck cancer: Ku80 expression predicts locoregional failure and death following radiotherapy. Clin Cancer Res 2011;17(7):2035–43.
[25] Wang S, Wang Z, Liu X, Liu Y, Jia Y. Overexpression of Ku80 suggests poor prognosis of locally advanced esophageal squamous cell carcinoma patients. World J Surg 2015;39(7):1773–81.
[26] Chandrashekar DS, Bashel B, Balasubramanya SAH, et al. UALCAN: a portal for facilitating tumor subgroup gene expression and survival analyses. Neoplasia 2017;19(8):649–58.
[27] Kummar S, Ji J, Morgan R, et al. A phase I study of veliparib in combination with metronomic cyclophosphamide in adults with refractory solid tumors and lymphomas. Clin Cancer Res 2012;18(6):1726–34.
[28] Sonnenblick A, de Azambuja E, Azim Jr HA, Piccart M. An update on PARP inhibitors–moving to the adjuvant setting. Nat Rev Clin Oncol 2015;12(1):27–41.
[29] Evans T, Matulonis U. PARP inhibitors in ovarian cancer: evidence, experience and clinical potential. Ther Adv Med Oncol 2017;9(4):253–67.
[30] Murai J, Huang SY, Das BB, et al. Trapping of PARP1 and PARP2 by clinical PARP inhibitors. Cancer Res 2012;72(21):5588–99.
[31] Barr AR, Cooper S, Heldt FS, et al. DNA damage during S-phase mediates the proliferation-quiescence decision in the subsequent G1 via p21 expression. Nat Commun 2017;8:14728.
[32] Schultz N, Lopez E, Saleh-Gohari N, Helleday T. Poly(ADP-ribose) polymerase (PARP-1) has a controlling role in homologous recombination. Nucleic Acids Res 2003;31(17):4959–64.
[33] Anders L, Guenther MG, Qi J, et al. Genome-wide localization of small molecules. Nat Biotechnol 2014;32(1):92–6.
[34] Delmore JE, Issa GC, Lemieux ME, et al. BET bromodomain inhibition as a therapeutic strategy to target c-Myc. Cell 2011;146(6):904–17.
[35] Ott CJ, Kopp N, Bird L, et al. BET bromodomain inhibition targets both c-Myc and IL7R in high-risk acute lymphoblastic leukemia. Blood 2012;120(14):2843–52.
[36] Zuber J, Shi J, Wang E, et al. RNAi screen identifies Brd4 as a therapeutic target in acute myeloid leukaemia. Nature 2011;478(7370):524–8.
[37] Arnold NB, Arkus N, Gunn J, Korc M. The histone deacetylase inhibitor suberoylanilide hydroxamic acid induces growth inhibition and enhances gemcitabine-induced cell death in pancreatic cancer. Clin Cancer Res 2007;13(1):18–26.
[38] Bruzzese F, Rocco M, Castelli S, Di Gennaro E, Desideri A, Budillon A. Synergistic antitumor effect between vorinostat and topotecan in small cell lung cancer cells is mediated by generation of reactive oxygen species and DNA damage-induced apoptosis. Mol Cancer Ther 2009;8(11):3075–87.
[39] Buck E, Eyzaguirre A, Brown E, et al. Rapamycin synergizes with the epidermal growth factor receptor inhibitor erlotinib in non-small-cell lung, pancreatic, colon, and breast tumors. Mol Cancer Ther 2006;5(11):2676–84.
[40] Durkin AJ, Bloomston PM, Rosemurgy AS, et al. Defining the role of the epidermal growth factor receptor in pancreatic cancer grown in vitro. Am J Surg 2003;186(5):431–6.
[41] Li T, Ling YH, Goldman ID, Perez-Soler R. Schedule-dependent cytotoxic synergism of pemetrexed and erlotinib in human non-small cell lung cancer cells. Clin Cancer Res 2007;13(11):3413–22.
[42] Pitts TM, Morrow M, Kaufman SA, Tentler JJ, Eckhardt SG. Vorinostat and bortezomib exert synergistic antiproliferative and proapoptotic effects in colon cancer cell models. Mol Cancer Ther 2009;8(2):342–9.
[43] Loven J, Hoke HA, Lin CY, et al. Selective inhibition of tumor oncogenes by disruption of super-enhancers. Cell 2013;153(2):320–34.
[44] Lenhart R, Kirov S, Desilva H, et al. Sensitivity of small cell lung Cancer to BET inhibition is mediated by regulation of ASCL1 gene expression. Mol Cancer Ther 2015;14(10):2167–74.
[45] Lam LT, Lin X, Faivre EJ, et al. Vulnerability of small-cell lung Cancer to apoptosis induced by the combination of BET Bromodomain proteins and BCL2 inhibitors. Mol Cancer Ther 2017;16(8):1511–20.
[46] Yang L, Zhang Y, Shan W, et al. Repression of BET activity sensitizes homologous recombination-proficient cancers to PARP inhibition. Sci Transl Med 2017;9(400).
[47] Murai J, Zhang Y, Morris J, et al. Rationale for poly(ADP-ribose) polymerase (PARP) inhibitors in combination therapy with camptothecins or temozolomide based on PARP trapping versus catalytic inhibition. J Pharmacol Exp Ther 2014;349(3):408–16.